Structural basis of oligomerization in septin-like GTPase of immunity-associated protein 2 (GIMAP2)

David Schwefel[a,b], Chris Fröhlich[a,b], Jenny Eichhorst[c], Burkhard Wiesner[c], Joachim Behlke[a], L. Aravind[d], and Oliver Daumke[a,e,1]

[a]Max-Delbrück-Centrum für Molekulare Medizin, Kristallographie, Robert-Rössle-Strasse 10, 13125 Berlin, Germany; [b]Institut für Chemie und Biochemie, Freie Universität Berlin, Takustrasse 3, 14195 Berlin, Germany; [c]Leibniz-Institut für Molekulare Pharmakologie, Robert-Rössle-Strasse 10, 13125 Berlin, Germany; [e]Institut für Medizinische Physik und Biophysik, Charité, Ziegelstrasse 5-9, 10117 Berlin, Germany; and [d]National Center for Biotechnology Information, National Library of Medicine, National Institutes of Health, Bethesda, MD 20894

Edited by Axel T. Brunger, Stanford University, Stanford, CA, and approved October 6, 2010 (received for review July 19, 2010)

GTPases of immunity-associated proteins (GIMAPs) are a distinctive family of GTPases, which control apoptosis in lymphocytes and play a central role in lymphocyte maturation and lymphocyte-associated diseases. To explore their function and mechanism, we determined crystal structures of a representative member, GIMAP2, in different nucleotide-loading and oligomerization states. Nucleotide-free and GDP-bound GIMAP2 were monomeric and revealed a guanine nucleotide-binding domain of the TRAFAC (translation factor associated) class with a unique amphipathic helix α7 packing against switch II. In the absence of α7 and the presence of GTP, GIMAP2 oligomerized via two distinct interfaces in the crystal. GTP-induced stabilization of switch I mediates dimerization across the nucleotide-binding site, which also involves the GIMAP specificity motif and the nucleotide base. Structural rearrangements in switch II appear to induce the release of α7 allowing oligomerization to proceed via a second interface. The unique architecture of the linear oligomer was confirmed by mutagenesis. Furthermore, we showed a function for the GIMAP2 oligomer at the surface of lipid droplets. Although earlier studies indicated that GIMAPs are related to the septins, the current structure also revealed a strikingly similar nucleotide coordination and dimerization mode as in the dynamin GTPase. Based on this, we reexamined the relationships of the septin- and dynamin-like GTPases and demonstrate that these are likely to have emerged from a common membrane-associated dimerizing ancestor. This ancestral property appears to be critical for the role of GIMAPs as nucleotide-regulated scaffolds on intracellular membranes.

G protein | protein structure

GTPases of immunity-associated proteins (GIMAPs) belong to a conserved clade of guanine nucleotide-binding (G) proteins found in various eukaryotes and certain bacteria and viruses (1, 2). In humans, the seven GIMAP genes are clustered on chromosome 7 and are predominantly expressed in lymphocytes (3). The encoded proteins have a molecular mass of 33–38 kD and are comprised of an amino (N-)terminal G domain containing a GIMAP-specific signature motif, the conserved box, followed by distinct carboxy-(C-)terminal extensions of 60–130 amino acids length. The 75-kD GIMAP8 differs in being composed of three consecutive GIMAP-specific G domains. Human GIMAP1, GIMAP2, and GIMAP5 have one or two additional hydrophobic segments at their C termini predicted to form transmembrane (TM) spanning helices. Sequence analysis indicated that GIMAPs belong to the TRAFAC (translation factor associated) class of GTPases, which are typified by an antiparallel β-strand at one end of the sheet (4). The beginning of this strand is associated with a highly conserved sensor threonine or serine that is in the heart of the switch I region (Fig. S1). Within the TRAFAC class, GIMAPs, together with the plant-specific Toc (translocon at the outer envelope membrane of chloroplasts) proteins, comprise a distinctive clade, which is closest to the septins. They typically contain a divergent version of the guanine recognition motif (G4) at the end of the core strand 5 (4) and an additional helix α6 at the C terminus of the GTPase domain (Fig. S1). Toc proteins function as integral components of the chloroplast protein import machinery (5). Septins in the budding yeast have been shown to assemble in rings along the bud neck and to function as a scaffold that organizes the assembly of binding partners. In vertebrates, septins are involved in cell division, cytoskeletal dynamics, and secretion (reviewed in ref. 6).

Studies in animals showed a drastic up-regulation of GIMAP expression during T cell development (7–9) and a function of GIMAPs in T cell selection processes. GIMAP3, GIMAP4, and GIMAP5 were shown to interact with members of the Bcl2 family and regulate apoptosis (8, 10). Several studies have established a role for GIMAPs in the late stages of lymphocyte development and in lymphocyte maintenance. A GIMAP5-deficient rat strain exhibits severe loss of peripheral T cells (lymphopenia) and develops spontaneous type I diabetes (11–13). GIMAP5 knockout mice have a similar phenotype, including lymphopenia, complete loss of natural killer cells, and death after 15 weeks, presumably due to liver failure (14). Conditional knockout of GIMAP1 in mouse lymphoid tissues resulted in an almost complete loss of mature B and T cells, highlighting the central function of GIMAPs in regulation of lymphocyte survival also in the B cell lineage (15). The role of GIMAPs in human diseases is underpinned by the observation that a single nucleotide polymorphism in GIMAP5 is associated with IA2 autoantibodies in type 1 diabetes (T1D) patients and systemic lupus erythematosus (16, 17). The expression of almost the whole GIMAP family is turned down in regulatory T cells of patients suffering from T1D (18). Furthermore, GIMAPs belong to the most down-regulated proteins in anaplastic large cell lymphomas compared to the progenitor T cells (19). In contrast, overexpression of GIMAPs was implicated in certain types of leukemia (20) and lung cancer (21).

To obtain functional and mechanistic insights into the GIMAP family and understand their role in human disease, we initiated a biochemical, structural, and cellular analysis for a representative GIMAP, GIMAP2.

Results

Structure of Monomeric GIMAP2. A human GIMAP2 construct lacking the two hydrophobic C-terminal segments (GIMAP2$^{1–260}$,

Author contributions: D.S., J.B., L.A., and O.D. designed research; D.S., C.F., J.B., and L.A. performed research; J.E., B.W., J.B., and L.A. contributed new reagents/analytic tools; D.S., C.F., J.B., L.A., B.W., and O.D. analyzed data; and D.S., L.A., and O.D. wrote the paper.

The authors declare no conflict of interest.

This article is a PNAS Direct Submission.

Data deposition: The atomic coordinates have been deposited in the Protein Data Bank, www.pdb.org [PDB ID codes 2xtp (GIMAP2$^{1–260}$), 2xto (GIMAP2$^{21–260}$•GDP), 2xtm (GIMAP2$^{1–234}$•GDP), and 2xtn (GIMAP2$^{1–234}$•GTP)].

[1]To whom correspondence should be addressed. E-mail: oliver.daumke@mdc-berlin.de.

This article contains supporting information online at www.pnas.org/lookup/suppl/doi:10.1073/pnas.1010322107/-/DCSupplemental.

BIOCHEMISTRY

Fig. 1*A*) was expressed in bacteria and purified to homogeneity (22). Using HPLC analysis we found that the purified protein was partially bound to GTP, which could be removed by an additional washing step with a magnesium chelator, EDTA (Fig. S2). This construct was crystallized in the absence of nucleotide, and the structure determined by a single-anomalous dispersion protocol using selenomethionine-substituted protein crystals (22) (Table S1).

The N-terminal 20 residues of GIMAP2 are disordered and not included in our model. Ser21 is right at beginning of the first strand of the G domain containing a central β-sheet sandwiched by two layers of α-helices (Fig. 1 *A* and *B* and Fig. S3). Consistent with previous sequence-based observations (4), a search of the Protein Data Bank (PDB) database with the GIMAP2 G domain using the DALIlite program recovers the chloroplast-membrane-associated Toc GTPases (e.g., PDB ID codes 2je3 and 1h65) as closest GIMAP relatives, and the structures can be superimposed with a rmsd of 2.8 Å over 186 aligned C_α positions at a sequence identity of ~17–18%. Within the core G domain, GIMAP2 displays an additional helix α3* between strand 5 and helix α4 (Fig. 1*B* and Fig. S4*A*)—the presence of an additional helix in this region is a feature also encountered in the septins and some of the dynamin-like GTPases (Fig. S1). Beyond the core G domain, the GIMAP2 structure shows a distinct C-terminal extension of two helices α6 and α7 (Fig. 1*B*). Also the Toc GTPases, septins, and members of the dynamin-like clade bear a C-terminal helix comparable to α6 (Fig. S1) (23–25). However, the GIMAP2 structure is distinguished by the amphipathic helix α7 that is located on the opposite face of the nucleotide-binding site. This helix is connected to the G domain by a disordered linker of 16 residues and directly contacts the switch II region of the G domain (Fig. 1*B*). Unlike both the Tocs and septins, the GIMAP2 structure lacks the characteristic β-hairpin insert between strand 6 and helix α5 (Figs. S1 and S4*A*).

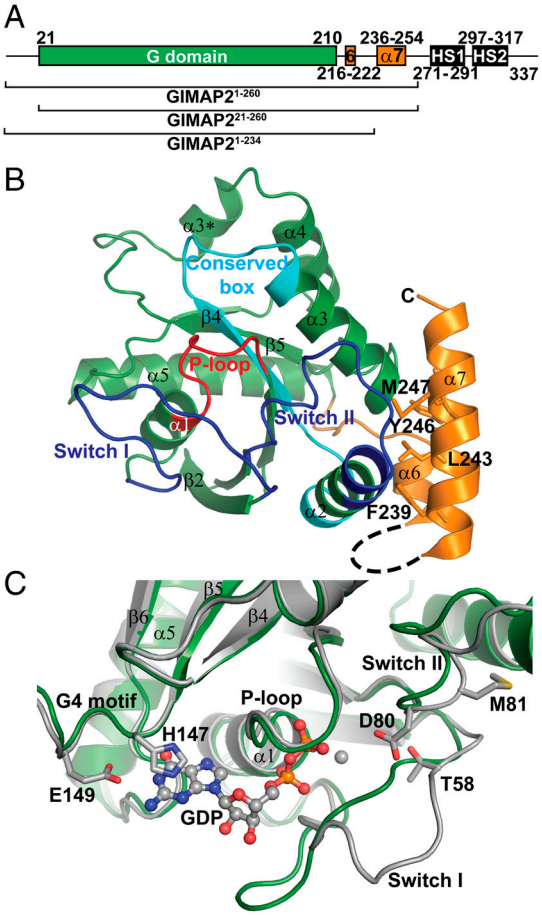

Fig. 1. The structure of monomeric GIMAP2. (*A*) Schematic representation of the domain structure of GIMAP2, with the amino acid positions indicated. The C-terminal extension is shown in orange and the two hydrophobic segments (HS1 and HS2) in black. Crystallized constructs are indicated below the scheme. (*B*) Cartoon representation of the nucleotide-free structure of GIMAP2$^{1–260}$. The G domain is shown in green, the two switch regions in blue, the *P* loop in red, and the conserved box in cyan. The C-terminal helices α6 and α7 are shown in orange, with the hydrophobic residues indicated as sticks. The disordered loop connecting helices α6 and α7 is indicated by a dashed line. (*C*) Details of GDP binding in the structure of GIMAP2$^{21–260}$•GDP (shown in gray). Selected residues in the nucleotide-binding motifs are shown as sticks. The magnesium ion is shown as gray sphere. Significant structural changes compared to the nucleotide-free structure (green) were observed in switch I.

To determine binding affinities of GIMAP2 to guanine nucleotides, isothermal titration calorimetry was used. GIMAP2 bound GTP with an equilibrium dissociation constant (K_d) of 40 nM and GDP with a K_d of 630 nM (Fig. S5*A*). However, GTP was not hydrolyzed, even during long incubations (>24 h) and at high protein concentration (50 μM) (see *Materials and Methods*). To obtain insights into the nucleotide-binding mode, a construct lacking the disordered N terminus, GIMAP2$^{21–260}$ (Fig. 1*A*), was crystallized in the GDP-bound form and the structure solved by molecular replacement (Table S1). Clear electron density was visible for the GDP molecule in the nucleotide-binding pocket (Fig. S5*B*). The overall structure of GIMAP2$^{21–260}$•GDP is very similar to the nucleotide-free form, except for significant structural changes observed in the switch I region (Fig. 1*C*). The guanine nucleotide-binding motifs G1–G5 of GIMAP2 show sequence differences compared to the canonical TRAFAC GTPases, but function in a similar manner in nucleotide binding (Fig. S4 *B* and *C*). Interestingly, the side chain of Asp80 in the G3 motif of GIMAP2 points toward the β-phosphate, whereas a glycine at the equivalent position acts as a sensor for the γ-phosphate in most other TRAFAC class GTPases, including the closely related Tocs and the more distantly related Ras (26). A glutamine or histidine residue positions the catalytic water molecule in Ras-like small GTPases, EF1/EF-TU, EF2/EF-G, eIF2, IF2, and SelB (27). However, in GIMAP2 it is replaced by a hydrophobic residue (Met81), just as in many members of the Toc, septin, dynamin-like, Era, and Eng GTPases (Fig. S1). Both GIMAP2 and the Toc GTPase contain a histidine in the second position of the G4 motif, in place of the usual lysine, which recognizes the guanine via a pi–pi stacking interaction between the histidine and guanine rings (Fig. 1*C*). Despite extensive screening efforts, no crystals were obtained for the described constructs in the GTP-bound form.

Oligomerization of GIMAP2. The C-terminal helix α7 in the nucleotide-free GIMAP2 structure had higher temperature (B) factors compared to the core G domain (Fig. S6*A*) suggesting increased flexibility in this helix. A construct lacking helix α7 (GIMAP2$^{1–234}$, Fig. 1*A*) was crystallized in the GDP- and GTP-bound form, and the structures were solved by molecular replacement (Table S1). Clear electron density for the nucleotides was present in both structures (Fig. S5 *C* and *D*) including the γ-phosphate in the GTP-bound structure, indicating that no GTP hydrolysis had occurred in the crystals.

GTP-bound GIMAP2$^{1–234}$ oligomerized via two distinct interfaces in the crystal (Fig. 2 *A*–*D*), with the C-terminal tails of the monomers pointing pairwise in opposite directions. Only in the GTP-, but not in the GDP-bound form of GIMAP2$^{1–234}$, a symmetric interface of 600 Å^2 was observed across the guanine nucleotide-binding site (the G interface, Fig. 2 *B* and *C*), which involves the conserved box, switch I, the specificity motif G4, and helix α3*. The highly conserved Arg117 from one GIMAP2 monomer forms a hydrogen bond across the G interface to

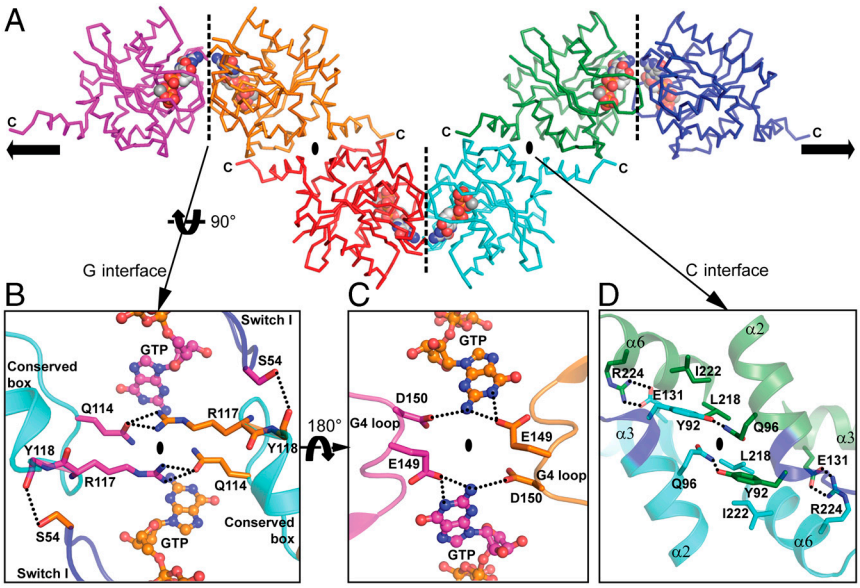

Fig. 2. Oligomerization of GIMAP2. (*A*) Ribbon representation of the GTP-bound GIMAP2$^{1–234}$ oligomer, with the nucleotides shown as space-filling models. The crystallographic twofold symmetry axes within the C (ellipse) and G interface (dotted line) are indicated. The indicated C-termini point in opposing directions in a pairwise manner. (*B*) Detailed view of the G interface with selected residues shown as sticks. The crystallographic twofold axis is shown as an ellipse. (*C*) GTP coordination in the oligomer. The exocyclic amino group of the guanine base forms hydrogen bonds to Glu149 *in cis* and to Asp150 *in trans* across the G interface. The crystallographic twofold axis is shown as an ellipse. (*D*) Detailed view of the C interface. The crystallographic twofold axis is shown as an ellipse.

Gln114 of the opposing monomer (both from the conserved box). The exocyclic amino group of the guanine base is directly involved in dimerization by forming a hydrogen bond to the highly conserved Asp150 in the G4 loop, directly following the G4 motif (Fig. 2*C* and Fig. S3). A strikingly similar interaction across the nucleotide-binding site has recently been reported for the dynamin G domain dimer where Asp211 from the G4 loop interacts *in trans* in the same fashion with the nucleotide (28). GTP sensing of the G interface is mediated by switch I. This region is stabilized by hydrogen bonds of Thr58 and a main chain contact of Leu57 to the γ-phosphate, which enables Ser54 to form a hydrogen bond to the main chain oxygen of Tyr118 of the opposing molecule (Figs. 2*B* and 3*A*).

To further study the relevance of the G interface in solution, the assembly status of GIMAP2 at different protein concentrations was determined by analytical ultracentrifugation (AUC) in the presence of GDP and GTP. GIMAP2$^{1–260}$ dimerized with low affinity only in the presence of GTP (K_d = 250 μM) (Fig. 3*B*). In contrast, mutations in switch I (S54A) and in the conserved box (R117D) in the G interface prevented GTP-dependent dimerization (Fig. 3*B*).

A second symmetric, mostly hydrophobic interface of 1100 Å^2, the C interface, was present at the C terminus of both GDP- and GTP-bound GIMAP2$^{1–234}$ structures (Fig. 2*D*). Helices α2 of switch II, α3, and α6 contribute residues to this interface. The C interface was created by removal of α7, which resulted in stable dimerization of the GIMAP2$^{1–234}$ construct, as shown by analytical gel filtration and AUC experiments (Fig. 3*C* and Fig. S6*B*). This construct further oligomerized with low affinity in the presence of GTP (Fig. S6*B*). In agreement with the involvement of helix α6 in the C interface, further shortening of this helix in the GIMAP2$^{1–223}$ construct resulted again in a monomeric form (Fig. 3*C*). Interestingly, stable dimerization after removal of helix α7 appears to be a general feature of membrane-anchored GIMAPs, because it was also observed for the corresponding GIMAP5 constructs (Fig. S6*C*).

Switch II does not participate in the G interface but is in direct contact with helix α7 and drastically changes its conformation upon GTP binding (Fig. 3*D*). Asp80 in the GDP-bound form points into the nucleotide-binding pocket, whereas it is expelled from this position in the GTP-bound form by the negatively charged γ-phosphate. Consequently, it flips out and interacts with His87. The resulting rearrangements in switch II induce a repositioning of Glu89, which prevents salt bridge formation to Lys240 in helix α7 (Fig. 3*D*). Our structural analysis therefore suggests that GTP-induced structural changes in switch II disrupt contacts between the G domain and helix α7 and weaken the affinity between these two elements. To exclude that the observed conformational changes in switch II were induced by removal of α7, we compared GDP-bound GIMAP2$^{1–234}$ and GDP-bound GIMAP2$^{21–260}$ and found that they adopt nearly identical conformations (Fig. S6*D*).

Cellular Localization of GIMAP2. To explore the cellular localization of GIMAP2, overexpression studies in a Jurkat T cell line were performed. mCherry-tagged full-length GIMAP2 localized to large spherical structures with a diameter of approximately 0.8 μm (Fig. 4*A*). These structures did not costain with markers of the endoplasmic reticulum (ER) (ER tracker), mitochondria (Mitotracker), lysosomes, or late endosomes (LAMP1). Based on a similar staining pattern recently reported for the mouse interferon-gamma induced GTPase Igtp in dendritic cells (29), we tested for costaining with the lipid droplet (LD) marker BODIPY 493/503 and indeed found colocalization with GIMAP2 (Fig. 4 *A* and *B*). The fluorescent GIMAP2 signal was enriched at the border of LDs (Fig. 4*B*), suggesting that GIMAP2 resides mainly at the phospholipid monolayer surrounding the LD core of neutral lipids, which is stained by BODIPY 493/503. The predicted C-terminal hydrophobic segments of GIMAP2 were necessary and sufficient for the reported localization, because deletion of these segments led to a cytoplasmic staining, and the hydrophobic segments on their own targeted the mCherry fluorescent protein to LDs (Fig. 4 *C* and *D*). We noticed that overexpression of mCherry-tagged full-length GIMAP2 in Jurkat cells induced a significant twofold increase of LD number per cell (average of 33 LDs per cell, Fig. 4*E*), compared to nontransfected cells and cells transfected with mCherry only (average of 15 or 12 LDs per cell, respectively, Fig. 4*E*). In contrast, overexpressed GIMAP2 point mutants in the G interface (R117D) or C interface (R224D) still localized to LDs but did not cause an increase of the LD number (Fig. 4*E*), suggesting a function of the GIMAP2 oligomer at the surface of LDs.

Discussion

Nucleotide-dependent oligomerization at membrane surfaces is a common theme in many G protein families, e.g., in the dynamins (30), the immunity-related GTPases (IRGs) (31) and the septin family (6). Fitting of nonoligomerized G protein components into low resolution electron microscopy reconstruction of the oligomeric assemblies yielded structural models for helical dynamin

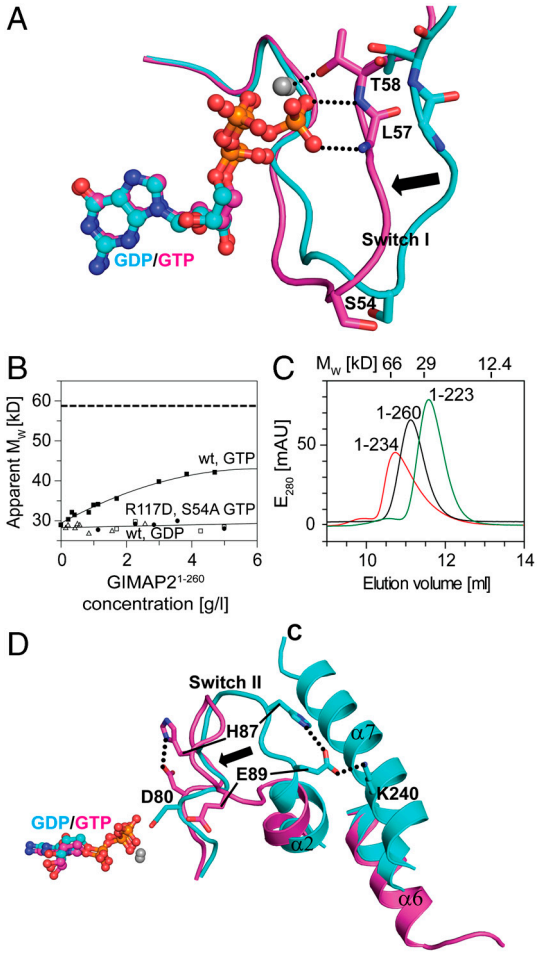

Fig. 3. Mechanistic insights into GIMAP oligomerization. (*A*) Superposition of GDP-bound GIMAP2$^{21–260}$ (cyan) and GTP-bound GIMAP2$^{1–234}$ (magenta) shows the rearrangement of switch I upon GTP binding, leading to dimerization across the G interface. The movement of switch I is indicated by the black arrow. Selected residues undergoing major conformational changes are shown as sticks. (*B*) Probing the G interface. Sedimentation equilibrium ultracentrifugation experiments for GIMAP2$^{1–260}$ in the presence of 100 μM GTP (■) and GDP (Δ) and for the GIMAP2$^{1–260}$ mutants R117D (□) and S54A (●) in the presence of 100 μM GTP were carried out to determine apparent molecular masses at different protein concentrations. A monomer–dimer equilibrium was fitted to GIMAP2$^{1–260}$ in the presence of GTP, resulting in $K_d = 250 \pm 20$ μM. The dashed line indicates the molecular mass of the GIMAP2 dimer. (*C*) Analytical gel filtration experiments for GIMAP2$^{1–234}$ (red), GIMAP2$^{1–260}$ (black), and GIMAP2$^{1–223}$ (green) show the involvement of helix α6 in dimerization across the C interface. Elution volumes of protein standards are indicated on top of the graph. (*D*) A superposition of GDP-bound GIMAP2$^{21–260}$ (cyan) and GTP-bound GIMAP2$^{1–234}$ (magenta) shows the rearrangements of switch II upon GTP binding. The movement of switch II is indicated by a black arrow. Selected residues undergoing major conformational changes are shown as sticks.

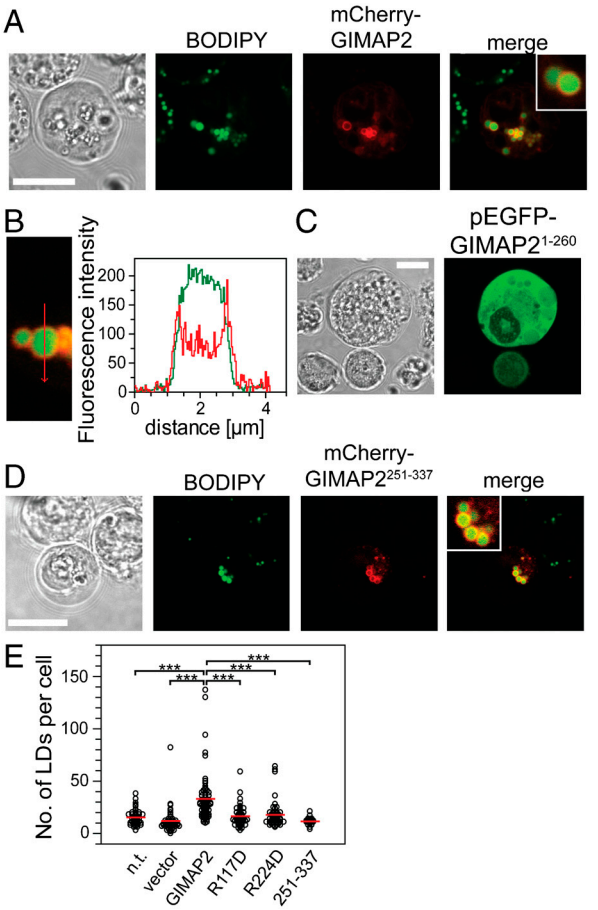

Fig. 4. Cellular localization of GIMAP2. (*A*) N-terminally mCherry-tagged GIMAP2 (red) was overexpressed in Jurkat cells and LDs were stained with BODIPY 493/503 (green). Living cells were analyzed by confocal fluorescence microscopy. All scale bars represent 10 μm. (*B*) Profile of the fluorescent signals across a LD (*Right*) along the indicated line (*Left*). (*C*) N-terminally EGFP-tagged GIMAP2$^{1–260}$ lacking the hydrophobic segments was overexpressed in Jurkat cells and analyzed by confocal microscopy. (*D*) The C-terminal hydrophobic segments of GIMAP2 (residues 251–337) were expressed as N-terminal mCherry fusion in Jurkat cells, costained with BODIPY 493/503 (green), and analyzed by confocal microscopy. (*E*) Quantification of LD number per cell. Jurkat cells were transfected with the indicated GIMAP2 constructs and the number of LDs determined using the BODIPY 493/503 stain in two independent experiments. n.t.—not transfected ($n = 45$), vector—transfected with pmCherry-C ($n = 48$). GIMAP2—transfected with pmCherry-C-GIMAP2 ($n = 69$). R117D—transfected with pmCherry-C-GIMAP2 R117D ($n = 48$). R224D—transfected with pmCherry-C-GIMAP2 R224D ($n = 49$). 251–337—transfected with pmCherry-C-GIMAP2$^{251–337}$ ($n = 17$). Only transfected cells were evaluated, as judged by inspection of the mCherry fluorescence. Red bars indicate the mean number of LDs per cell. Three asterisks represent $P < 0.0001$ according to Wilcoxon–Mann–Whitney test (47). See also Fig. 2 *B* and *D*, where the role of the mutated amino acid residues R117 and R224 in GIMAP2 oligomerization is indicated.

(32, 33) and bacterial dynamin-like protein oligomers (34). Mutagenesis-based modeling was employed to deduce the structure of the ring-like dynamin-related EHD2 oligomer (35). Only in rare cases, linear oligomers were compatible with crystal formation, e.g., in the case of the linear septin oligomer (25) or the stalk of the antiviral MxA GTPase (33).

In the present work, we describe high-resolution structures of monomeric and oligomerized GIMAP2 constructs that elucidate the mechanism of nucleotide-mediated oligomerization in the GIMAP family. GTP-induced stabilization of switch I leads to low affinity dimerization of GIMAP2 via the G interface. Such low affinity interaction is typical for proteins that are locally concentrated on a membrane surface and thereby restricted in their mobility (36, 37). Switch II, on the other hand, is not involved in the G interface, unlike in the corresponding G interfaces of septin2 (25), Toc34 (23, 24), and dynamin (28) (Fig. S1). Our structural analysis suggests that switch II of GIMAP2 instead controls the association of the G domain with helix α7, with Asp80 acting as γ-phosphate sensor. We suggest that in the presence of a suitable acceptor substrate such as membrane or an interaction partner, α7 is released from the G domain in a GTP-dependent fashion and oligomerization proceeds via the C interface. A similar scenario has been suggested for the charged multivesicular body proteins (CHMPs) involved in multivesicular body genesis, where an autoinhibitory C-terminal amphipathic helix

prevents oligomerization on the membrane surface (38). Furthermore, Arf and Sar GTPases release an N-terminal helix upon GTP binding that inserts into the membrane and induces membrane remodeling (39, 40). The amphipathic helix α7 might also interact with binding partners of GIMAPs, e.g., Bcl2 family members, which are known to associate with each other via amphipathic helices that bind into a hydrophobic acceptor groove (41), and this interaction is strongly promoted in the presence of membranes (42). The C interface of GIMAPs is unique leading to a different architecture of the oligomer compared to septins (25) and dynamin/MxA (33).

GIMAP2 is a lymphocyte-specific LD component. Targeting of GIMAP2 to LDs is mediated by its two C-terminal hydrophobic segments. The presence of two such segments distinguishes GIMAP2 from other human GIMAPs or GIMAP orthologues in mice and rat. Human GIMAP1 and GIMAP5 contain one predicted C-terminal transmembrane helix (Fig. S3) and have been found at different subcellular compartments, e.g., the Golgi apparatus and lysosomes, respectively (43). On the other hand, LD targeting of caveolin and other proteins is mediated via long hydrophobic regions, which might insert as hairpins into the LD monolayer and which do not share sequence similarity to the hydrophobic segments of GIMAP2 (44). Furthermore, our overexpression experiments employing wild-type and mutant GIMAP2 suggest a role of the GIMAP2 oligomer in LD formation. It is tempting to speculate that the function of the oligomer is related to cross-linking of LDs to each other or to their source membrane. This is supported by the architecture of the GIMAP2 oligomer with its C-terminal tails pointing in opposing directions. At the same time, the GIMAP2 oligomer might act as a scaffold to assemble interaction partners on the LD membrane.

The dimerization mode of GIMAP2 via the G interface is shared with the dynamin, Toc, and septin GTPases, with the associating G domains arranged in a similar head-to-head orientation (Figs. S1 and S7) (45). Corresponding regions of the respective G domains are used to build up the dimer, which are switch I, the GIMAP conserved box (equivalent to the "*trans* stabilizing loop" in dynamin 1 and the loop encompassing residues 154–163 in mouse septin 2), and the G4 loop, which in GIMAP2 and dynamin coordinates the nucleotide base *in trans* in a strikingly similar fashion. For dynamin and septin G domain dimers, further elements strengthen the G-interface interaction, namely switch II, the "dynamin-specific loop" or the septin-/Toc specific β7–β8 insertion. We used the structural information on GIMAP2 to reanalyze higher-order evolutionary relationships of GTPases and how versions that operate on the membrane might have emerged from an ancestral TRAFAC class GTPase involved in translation-related functions. Previous sequence–structure analysis suggested that the septins, Tocs, and GIMAPs are further related to GTPases of the Era family, which bind single-stranded 16S rRNA via their C-terminal KH domains and mediate the assembly of the 30S ribosomal subunit (46). Structures of GIMAP2, along with those of the Tocs, strongly support this relationship despite relatively low sequence similarity. To systematically assess the higher-order relationships between these G proteins, we created a relationship network connecting pairs of G protein structures by edges representing best hits in DALIlite structure–comparison searches, profile–profile comparisons, best pairwise alignment of dimers,

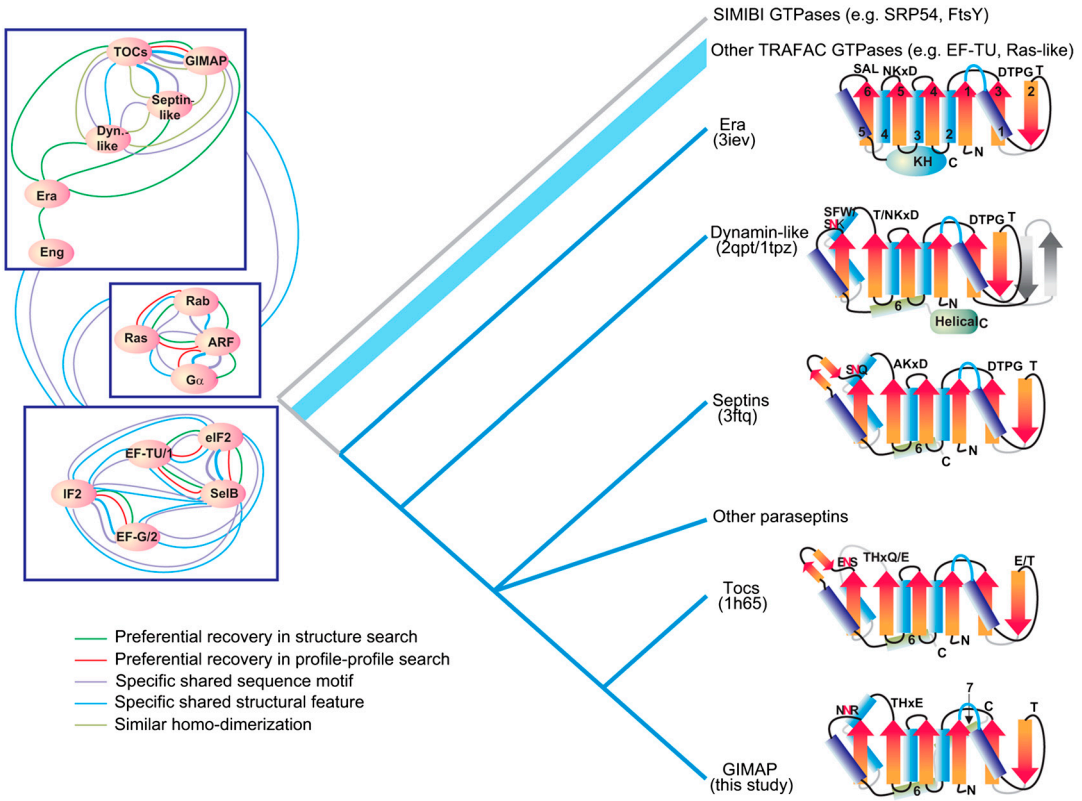

Fig. 5. Higher-order relationship analysis of the GIMAP family. (*Left*) The relationship network constructed based on different lines of evidence. The relative thickness of the edges between the nodes in the case of the specific sequence and structure features reflects the relative number of such features that are shared. At the higher level the major groups are boxed for simplicity of illustration, and the edges between them (i.e., those that define the TRAFAC class of GTPases) are shown. (*Right*) The inferred higher-order relationships as a cladogram, along with the simplified topologies of representative members of each clade for which structures are available (see PDB ID codes). For the dynamins a reconstructed structure of the ancestral version is depicted based on the two derived versions of the clade typified by EHD2 (PDB ID code 2QPT) and IIGP (PDB ID code 1TPZ). Also indicated on the topology are the typical forms of the different conserved GTPase motifs in a given group. The *P* loop is colored blue. The strands and helices are numbered in the Era structure, with the additional helices indicated in the structures in which they occur.

shared unique structural motifs, and specific conserved residue patterns (Fig. 5). As a result we were able to identify a distinct cluster of TRAFAC GTPases, which in addition to the above-mentioned proteins, also includes the dynamins. Previously, the point of origin of the dynamin-like proteins was not entirely clear—but their dimerization mode, the residues interacting with guanine in the G5 motif (including a characteristic Asn found in several members of the dynamin-like group) and other distinctive structural features (see above) suggest that they belong to the same higher-order clade. Furthermore, this relationship network suggests that Tocs and GIMAPs are the closest sister groups. The septins and dynamin-like proteins are successive sister groups to this clade, with all of them in turn being related to Era, to the exclusion of other TRAFAC class GTPases.

In terms of phyletic patterns, Era is most broadly distributed and plays an important role in assembly of the translation machinery in bacteria, eukaryotes, and some archaea. However, the remaining members of the above-mentioned group show a more sporadic distribution, especially the GIMAPs. Hence, it is conceivable that they emerged later from the more widely distributed regulators of the translation machinery. Further, they are all unified not only by their dimerization mode, but also by the fact that they often tend to associate with lipid membranes and perform functions related to it. Hence, it is reasonable to infer that the common ancestor of the GIMAPs, Tocs, and septin-like and dynamin-like GTPase evolved a distinctive membrane-binding mode via dimerization. However, each group appears to have evolved certain distinctive specializations that are reflected in their structure and sequence. In this regard it is interesting to note that both septins and Tocs, which are closer to the GIMAPs, share the unique β-hairpin insert after the G5 motif. This suggests that the GIMAPs lost this motif, whereas they acquired the α7 helix that is unique to them. This modification probably was critical for the emergence of their GTP-dependent interaction with the membrane or functional partners.

Materials and Methods

Protein expression, purification, and crystallization were carried out as described before (22). A detailed description of the biochemical experiments, structure solution, refinement, microscopy, and GTPase higher-order relationship analysis can be found in *SI Text*.

ACKNOWLEDGMENTS. We acknowledge advice and assistance by O. Ristau and C. Schilling (analytical ultracentrifugation analysis), K. Köchert and S. Mathas (cell culture), S. Werner and M. Papst (technical assistance), and the Berliner Elektronenspeicherring-Gesellschaft für Synchrotronstrahlung II staff at BL14.1, especially U. Müller (data collection and processing). O.D. acknowledges support by a Career Development Award of "The International Human Frontier Science Program Organization." L.A. is supported by the intramural funds of the National Institutes of Health.

1. Reuber TL, Ausubel FM (1996) Isolation of Arabidopsis genes that differentiate between resistance responses mediated by the RPS2 and RPM1 disease resistance genes. *Plant Cell* 8:241–249.
2. Poirier GM, et al. (1999) Immune-associated nucleotide-1 (IAN-1) is a thymic selection marker and defines a novel gene family conserved in plants. *J Immunol* 163:4960–4969.
3. Krucken J, et al. (2004) Comparative analysis of the human gimap gene cluster encoding a novel GTPase family. *Gene* 341:291–304.
4. Leipe DD, Wolf YI, Koonin EV, Aravind L (2002) Classification and evolution of *P*-loop GTPases and related ATPases. *J Mol Biol* 317:41–72.
5. Oreb M, Tews I, Schleiff E (2008) Policing Tic 'n' Toc, the doorway to chloroplasts. *Trends Cell Biol* 18:19–27.
6. Weirich CS, Erzberger JP, Barral Y (2008) The septin family of GTPases: Architecture and dynamics. *Nat Rev Mol Cell Biol* 9:478–489.
7. Baldwin TA, Hogquist KA (2007) Transcriptional analysis of clonal deletion in vivo. *J Immunol* 179:837–844.
8. Nitta T, et al. (2006) IAN family critically regulates survival and development of T lymphocytes. *PLoS Biol* 4:e103.
9. Dion C, et al. (2005) Expression of the Ian family of putative GTPases during T cell development and description of an Ian with three sets of GTP/GDP-binding motifs. *Int Immunol* 17:1257–1268.
10. Pandarpurkar M, et al. (2003) Ian4 is required for mitochondrial integrity and T cell survival. *Proc Natl Acad Sci USA* 100:10382–10387.
11. Hornum L, Romer J, Markholst H (2002) The diabetes-prone BB rat carries a frameshift mutation in Ian4, a positional candidate of Iddm1. *Diabetes* 51:1972–1979.
12. Macmurray AJ, et al. (2002) Lymphopenia in the BB rat model of type 1 diabetes is due to a mutation in a novel immune-associated nucleotide (Ian)-related gene. *Genome Res* 12:1029–1039.
13. Moralejo DH, et al. (2003) Genetic dissection of lymphopenia from autoimmunity by introgression of mutated Ian5 gene onto the F344 rat. *J Autoimmun* 21:315–324.
14. Schulteis RD, et al. (2008) Impaired survival of peripheral T cells, disrupted NK/NKT cell development, and liver failure in mice lacking Gimap5. *Blood* 112:4905–4914.
15. Saunders A, et al. (2010) Putative GTPase GIMAP1 is critical for the development of mature B and T lymphocytes. *Blood* 115:3249–3257.
16. Shin JH, et al. (2007) IA-2 autoantibodies in incident type I diabetes patients are associated with a polyadenylation signal polymorphism in GIMAP5. *Genes Immun* 8:503–512.
17. Hellquist A, et al. (2007) The human GIMAP5 gene has a common polyadenylation polymorphism increasing risk to systemic lupus erythematosus. *J Med Genet* 44:314–321.
18. Jailwala P, et al. (2009) Apoptosis of CD4+ CD25(high) T cells in type 1 diabetes may be partially mediated by IL-2 deprivation. *PLoS One* 4:e6527.
19. Eckerle S, et al. (2009) Gene expression profiling of isolated tumour cells from anaplastic large cell lymphomas: Insights into its cellular origin, pathogenesis and relation to Hodgkin lymphoma. *Leukemia* 23:2129–2138.
20. Zenz T, et al. (2004) hIan5: The human ortholog to the rat Ian4/Iddm1/lyp is a new member of the Ian family that is overexpressed in B-cell lymphoid malignancies. *Genes Immun* 5:109–116.
21. Taniwaki M, et al. (2006) Gene expression profiles of small-cell lung cancers: Molecular signatures of lung cancer. *Int J Oncol* 29:567–575.
22. Schwefel D, Fröhlich C, Daumke O (2010) Purification, crystallization and preliminary X-ray analysis of human GIMAP2. *Acta Crystallogr F* 66:725–729.
23. Sun YJ, et al. (2002) Crystal structure of pea Toc34, a novel GTPase of the chloroplast protein translocon. *Nat Struct Biol* 9:95–100.
24. Koenig P, et al. (2008) The GTPase cycle of the chloroplast import receptors Toc33/Toc34: Implications from monomeric and dimeric structures. *Structure* 16:585–596.
25. Sirajuddin M, et al. (2007) Structural insight into filament formation by mammalian septins. *Nature* 449:311–315.
26. Wittinghofer A, Pai EF (1991) The structure of Ras protein: A model for a universal molecular switch. *Trends Biochem Sci* 16:382–387.
27. Schweins T, et al. (1995) Substrate-assisted catalysis as a mechanism for GTP hydrolysis of p21ras and other GTP-binding proteins. *Nat Struct Biol* 2:36–44.
28. Chappie JS, Acharya S, Leonard M, Schmid SL, Dyda F (2010) G domain dimerization controls dynamin's assembly-stimulated GTPase activity. *Nature* 465:435–440.
29. Bougneres L, et al. (2009) A role for lipid bodies in the cross-presentation of phagocytosed antigens by MHC class I in dendritic cells. *Immunity* 31:232–244.
30. Praefcke GJ, McMahon HT (2004) The dynamin superfamily: Universal membrane tubulation and fission molecules? *Nat Rev Mol Cell Biol* 5:133–147.
31. Bekpen C, et al. (2005) The interferon-inducible p47 (IRG) GTPases in vertebrates: Loss of the cell autonomous resistance mechanism in the human lineage. *Genome Biol* 6:R92.
32. Mears JA, Ray P, Hinshaw JE (2007) A corkscrew model for dynamin constriction. *Structure* 15:1190–1202.
33. Gao S, et al. (2010) Structural basis of oligomerization in the stalk region of dynamin-like MxA. *Nature* 465:502–506.
34. Low HH, Sachse C, Amos LA, Lowe J (2009) Structure of a bacterial dynamin-like protein lipid tube provides a mechanism for assembly and membrane curving. *Cell* 139:1342–1352.
35. Daumke O, et al. (2007) Architectural and mechanistic insights into an EHD ATPase involved in membrane remodelling. *Nature* 449:923–927.
36. Katsamba P, et al. (2009) Linking molecular affinity and cellular specificity in cadherin-mediated adhesion. *Proc Natl Acad Sci USA* 106:11594–11599.
37. Schmid EM, McMahon HT (2007) Integrating molecular and network biology to decode endocytosis. *Nature* 448:883–888.
38. Muziol T, et al. (2006) Structural basis for budding by the ESCRT-III factor CHMP3. *Dev Cell* 10:821–830.
39. Lee MC, et al. (2005) Sar1p N-terminal helix initiates membrane curvature and completes the fission of a COPII vesicle. *Cell* 122:605–617.
40. Pucadyil TJ, Schmid SL (2009) Conserved functions of membrane active GTPases in coated vesicle formation. *Science* 325:1217–1220.
41. Petros AM, Olejniczak ET, Fesik SW (2004) Structural biology of the Bcl-2 family of proteins. *Biochim Biophys Acta* 1644:83–94.
42. Garcia-Saez AJ, Ries J, Orzaez M, Perez-Paya E, Schwille P (2009) Membrane promotes tBID interaction with BCL(XL). *Nat Struct Mol Biol* 16:1178–1185.
43. Wong VWY, et al. (2010) The autoimmunity-related GIMAP5 GTPase is a lysosome-associated protein. *Self/Nonself* 1:259–268.
44. Thiele C, Spandl J (2008) Cell biology of lipid droplets. *Curr Opin Cell Biol* 20:378–385.
45. Gasper R, Meyer S, Gotthardt K, Sirajuddin M, Wittinghofer A (2009) It takes two to tango: Regulation of G proteins by dimerization. *Nat Rev Mol Cell Biol* 10:423–429.
46. Tu C, et al. (2009) Structure of ERA in complex with the 3′ end of 16S rRNA: Implications for ribosome biogenesis. *Proc Natl Acad Sci USA* 106:14843–14848.
47. Wilcoxon F (1945) Individual comparisons by ranking methods. *Biometrics Bull* 1:80–83.